Received: 6 June 2017 | Revised: 16 October 2017 | Accepted: 15 February 2018
DOI: 10.1002/eco.1953

RESEARCH ARTICLE

WILEY

A physical framework for evaluating net effects of wet meadow restoration on late-summer streamflow

Caroline S. Nash[1] | **John S. Selker**[2] | **Gordon E. Grant**[3] | **Sarah L. Lewis**[1] | **Paul Noël**[4]

[1] College of Earth, Ocean, and Atmospheric Sciences, Oregon State University, Corvallis, OR, USA

[2] Department of Biological and Ecological Engineering, Oregon State University, Corvallis, OR, USA

[3] Pacific Northwest Research Station, USDA Forest Service, Corvallis, OR, USA

[4] Robert B. Daugherty Institute, University of Nebraska, Lincoln, NE, USA

Correspondence
Caroline S. Nash, College of Earth, Ocean, and Atmospheric Sciences, Oregon State University, USA.
Email: nashca@oregonstate.edu

Funding information
U.S. Department of the Interior Northwest Climate Science Center; U.S. Department of Agriculture Northwest Climate Hub

Abstract

Restoration of degraded wet meadows found on upland valley floors has been proposed to achieve a range of ecological benefits, including augmenting late-season streamflow. There are, however, few field and modelling studies documenting hydrologic changes following restoration that can be used to validate this expectation, and published changes in groundwater levels and streamflow following restoration are inconclusive. Here, we assess the streamflow benefit that can be obtained by wet-meadow restoration using a physically based quantitative analysis. This framework employs a 1-dimensional linearized Boussinesq equation with a superimposed solution for changes in storage due to groundwater upwelling and evapotranspiration, calculated explicitly using the White method. The model and assumptions gave rise to predictions in good agreement with field data from the Middle Fork John Day watershed in Oregon, USA. While raising channel beds can increase total water storage via increases in water table elevation in upland valley bottoms, the contributions of both lateral and longitudinal drainage from restored floodplains to late-summer streamflow were found to be undetectably small, while losses in streamflow due to greater transpiration, lower hydraulic gradients, and less laterally drainable pore volume were likely to be substantial. Although late-summer streamflow increases should not be expected as a direct result of wet-meadow restoration, these approaches offer benefits for improving the quality and health of riparian and meadow vegetation that would warrant considering such measures, even at the cost of increased water demand and reduced streamflow.

KEYWORDS

hydrology, incised channels, late-summer streamflow, stream restoration, wet meadow

1 | INTRODUCTION AND BACKGROUND

The restoration of wet meadows has persisted as a priority for land managers in semiarid and montane environments for over a quarter century (Ratliff, 1985; Benoit & Wilcox, 1997; Lindquist & Wilcox, 2000; Bernhardt et al., 2005; Tague, Valentine, & Kotchen, 2008; Hammersmark, Rains, & Mount, 2008). The impetus for restoration has gained new urgency as declining snowpack in montane environments (Nolin & Daly, 2006; Payne, Wood, Hamlet, Palmer, & Lettenmaier, 2004; Safeeq et al., 2015; Safeeq, Grant, Lewis, & Tague, 2013), which has been linked to changes in the timing and overall reductions in streamflow (Cayan, Dettinger, Kammerdiener, Caprio, & Peterson, 2001; Knowles & Cayan, 2002; Safeeq et al., 2013; Seager & Vecchi, 2010; Stewart, Cayan, & Dettinger, 2004; Tague & Grant, 2009) has prompted broader consideration of other potential sources of water storage whose release might augment summer streamflow (Barnett, Adam, & Lettenmaier, 2005; Barnett et al., 2008; Palmer et al., 2009; Poff, 2002). Restoring incised and often ephemeral stream channels back to wet meadows in montane environments has been proposed as one such source of late season water (Lindquist & Wilcox, 2000; Loheide & Gorelick, 2006; NFWF, 2010; Podolak et al., 2015; Tague et al., 2008; USDA, 2013).

The term *wet meadow* often comprises a range of wetland and semiwetland types but typically refers to herbaceous, groundwater dependent ecosystems that span broad, low-gradient alluvial valley bottoms composed of fine-grained sediments that maintain a shallow water table, commonly in montane environments (Fryjoff-Hung & Viers, 2013; Loheide, 2008; Ratliff, 1985; Wood, 1975). Unlike surrounding forests and shrubbed uplands, wet meadows exist as

Correction added on 25 May 2018 after initial online publication. The measurement units/values has been converted from cm to mm.

unique, water-rich environments that provide habitat for meadow-endemic species and forage for native ungulates (Allan-Diaz, 1991; Ratliff, 1985). Though the specific hydrogeomorphic conditions giving rise to wet meadows vary, they are most typically either fed directly by groundwater flowing in from the shallow subsurface of surrounding hillslopes (stratigraphic slope wetlands) or by local surface expressions of hillslope groundwater (topographic slope wetlands) (Brinson, 1993; Loheide, 2008).

As groundwater-dependent ecosystems, the plant communities populating wet meadows are uniquely sensitive to changing water table dynamics caused by both anthropogenic and natural geomorphic change (Allan-Diaz, 1991; Germanoski & Miller, 2004; Loheide, 2008; Lowry & Loheide, 2010; Ratliff, 1985). The rapid lowering of channel beds relative to adjacent floodplains or meadows has been well documented in meadows throughout the Sierra Nevada and is common throughout the Intermountain West (Bull, 1997; Ratliff, 1985). This channel incision (or gully erosion) has led to an increase in the water table depths beneath valley bottoms and has, in some locations, caused a dramatic shift in vegetation from hydric and mesic species towards xeric species better able to access deeper water (Ratliff, 1985; Allan-Diaz, 1991; Loheide & Gorelick, 2005, 2006, 2007; Cooper, Sanderson, Stannard, & Groeneveld, 2006; Hammersmark et al., 2008; Loheide et al., 2009).

The desiccation of these unique, water-rich environments has motivated interest in their restoration, often with the objective of generally improving hydrologic conditions (Benoit & Wilcox, 1997; Hammersmark et al., 2008; Rosgen, 1997). The specific techniques used to accomplish wet-meadow restoration vary but can be broadly classified between two end members: (a) the entire incised channel is filled with sediment and other material, and a new, smaller and typically more sinuous channel is constructed on the adjacent valley floor (e.g., plug and pond restoration) (Benoit & Wilcox, 1997; Hammersmark et al., 2008; Henery et al., 2011; Lindquist & Wilcox, 2000; Loheide & Gorelick, 2005; Ramstead, Allen, & Springer, 2012; Readle, 2014; Rosgen, 1997); and (b) the incised channel is partially or completely dammed with multiple low-head structures made of various materials (e.g., willow, logs, and rock) as a means of holding back water within the existing incised channel (Abbe & Brooks, 2013; Beechie et al., 2010; Harvey & Watson, 1986; Pollock et al., 2014; Roni, Hanson, & Beechie, 2008; Shields, Knight, & Cooper, 1995). The latter end member includes structures that mimic or derive inspiration from beaver dams, which while growing in popularity (Pilliod et al., 2018), will not be discussed specifically in this paper.

The unifying premise of these strategies is that raising the channel bed, and thus, the water surface elevation will (a) increase groundwater storage and reduce the depth to the water table which will (b) support the recovery of wet-meadow plant assemblages and (c) attenuate floodpeaks so that they slowly drain through the summer and augment baseflow. (Hammersmark et al., 2008; Heede, 1979; Liang et al., 2007; Loheide & Gorelick, 2007; NFWF, 2010; Podolak et al., 2015; Ponce & Lindquist, 1990; Swanson, Franzen, & Manning, 1987; Tague et al., 2008). Previous research has established that, in most circumstances, these restoration strategies are effective at accomplishing the first two goals. Both field data and hydrologic models indicate that the depth to the water table is typically reduced following restoration. The magnitude of the change is a function of the restored channel geomorphology (Loheide & Gorelick, 2007; Tague et al., 2008), soil media properties (Loheide et al., 2009; Essaid & Hill, 2014), local groundwater dynamics (Essaid & Hill, 2014), and spatiotemporal patterns in snowmelt (Lowry, Deems, Loheide, & Lundquist, 2010; Lowry & Loheide, 2010; Lowry, Loheide, Moore, & Lundquist, 2011). The effect will also vary seasonally, with larger post-restoration changes during active snowmelt and smaller changes in the late summer and early fall (Tague et al., 2008). In one field study, no change in the depth to water table was documented (Klein, Clayton, Alldredge, & Goodwin, 2007).

The reduced water table depths and associated increases in floodplain inundation have been linked to well-documented shifts in vegetation from scattered xeric or mesic species to dense hydric or mesic species (Allan-Diaz, 1991; Hammersmark et al., 2008; Hammersmark, Rains, Wickland, & Mount, 2009; Klein et al., 2007; Loheide & Gorelick, 2007; Tague et al., 2008). This is due, in part, to the increased availability of groundwater for root water uptake and transpiration (Lowry & Loheide, 2010). The hydrologic fingerprint of this vegetative change is a near doubling of the restored meadow's total evapotranspirative (ET) use (Loheide & Gorelick, 2005), increased maximum daily ET rate, and a later season peak daily ET (Hammersmark et al., 2008).

It is less clear whether the demonstrated increases in groundwater storage translate to increased streamflow, particularly in the late summer months when the majority of streamflow in channels is baseflow. Tague et al. (2008) have some of the only field data documenting the change, and while they report a postrestoration increase in streamflow during hydrograph recession, their statistical analysis shows a statistically insignificant decrease in streamflow during late summer. Watershed simulations aiming to further control for serial correlation and variability inherent to field data have reported both declines (Essaid & Hill, 2014; Hammersmark et al., 2008; Hammersmark, Dobrowski, Rains, & Mount, 2010) and increases in streamflow (Ohara et al., 2014).

We must be able to reasonably define expected outcomes of wet--meadow restoration if it is to remain a viable method of ecohydrologic restoration. The objective of this paper is to develop a generally applicable strategy to evaluate whether and how much streamflow is generated by the restoration of incised channels to wet meadows. In so doing, we aim to provide practitioners with a tool by which to set reasonable expectations when planning restoration projects.

2 | METHODS

To evaluate wet-meadow restoration's influence on late-summer streamflow, we employ a water budget framework to identify fluxes directly responsible for changes to water output following restoration. We go on to develop a physically based model of those fluxes and incorporate hillslope groundwater inputs and evapotranspirative use with a reformulation of the White method (Lautz, 2007; Loheide & Gorelick, 2005; White, 1932). We then briefly discuss the selection of parameters to maximize potential outputs within the constraints of realistic meadow conditions.

2.1 | Identifying significant fluxes using a water budget approach

To determine the potential contribution of meadow restoration to streamflow, we first consider the water budget for an unrestored upland valley floor (superscript *U* specifies an unrestored valley floor; subscripts specify direction of flow in or out of the valley floor system):

$$Q^U_{S,out} = \left(Q^U_{S,in} + GW^U_{in} + P * A\right) - \left(GW^U_{out} + ET^U * A\right) - \Delta S^U, \quad (1)$$

where Q_S (L^3/t) represents surface water (channelized and unchannelized), *GW* (L^3/t) represents groundwater fluxes through confined and unconfined aquifers, *P* (L/t) is precipitation, *A* (L^2) is valley floor area, *ET* (>0; L/t) is evapotranspiration from the valley floor vegetation and open water, and ΔS (L^3/t) reflects changes in valley water storage. When ΔS is positive, the valley is filling with water; when ΔS is negative, previously stored volumes of water are being depleted. Streamflow is typically largest when inputs exceed outputs, and the storage has been filled to capacity ($\Delta S = 0$; e.g., early spring melt in a snow dominated climate). As precipitation dwindles and evapotranspirative use rises, outputs may exceed inputs, causing storage to drain ($-\Delta S$). The reducing stores of water may be used to support increased evapotranspirative demand or may drain into an open channel as streamflow.

In the context of meadow restoration, it is useful to split groundwater into three component fluxes: water flowing through saturated and unsaturated sediments in the valley fill (GW_{VF}); water flowing in from both the saturated and unsaturated zones off hillslopes (GW_{HS}); and water in deep, confined aquifers (Figure 1). For the purposes of this analysis, we assume that changes to deep GW fluxes as a result of restoration are negligible. Henceforth, the term *groundwater* will only refer to inflow from hillslopes and water moving through the saturated and unsaturated porous media comprising the valley fill.

Surface and groundwater are often tightly linked in upland valley systems, and both are of interest for downstream users. It is therefore useful to combine surface water with water flowing through saturated and unsaturated valley fill into a single output term: valley discharge ($Q_{V,out}$)

$$Q^U_{V,out} = Q^U_{S,out} + GW^U_{VF,out} = \left(Q^U_{S,in} + GW_{HS} + P * A\right) - \left(ET^U * A\right) - \Delta S^U. \quad (2)$$

While the combined term effectively represents all water outputs available for downstream water users, it is important to note that groundwater leaving the restored valley may not be accessible downstream without mechanized extraction.

The water budget for a restored meadow follows similarly, with superscript *R* specifying a restored valley floor:

$$Q^R_{V,out} = Q^R_{S,out} + GW^R_{VF,out} = \left(Q^R_{S,in} + GW_{HS} + P * A\right) - \left(ET^R * A\right) - \Delta S^R. \quad (3)$$

The difference in outflowing valley water between the restored and unrestored upland valley floor can therefore be represented as the difference between these two budgets:

$$\begin{aligned} \Delta Q_{V,out} &= Q^R_{V,out} - Q^U_{V,out} \\ &= \left(Q^R_{inputs} - ET^R * A - \Delta S^R\right) - \left(Q^U_{inputs} - ET^U * A - \Delta S^U\right) \\ &= \left(Q^R_{inputs} - Q^U_{inputs}\right) + A\left(ET^U - ET^R\right) + \left(\Delta S^U - \Delta S^R\right). \end{aligned} \quad (4)$$

We assume that meadow restoration will not impact the magnitude of water inputs, reducing this relationship to

$$\Delta Q_{V,out} = A\left(ET^U - ET^R\right) + \left(\Delta S^U - \Delta S^R\right). \quad (5)$$

It is apparent that any net positive changes in summer-time outgoing valley water due to restoration would be due to reductions in evapotranspirative use and/or increases in delivery from valley-floor storage to the stream. As meadow restoration often aims to increase vegetative vigour, evapotranspiration should increase following restoration (Loheide & Gorelick, 2005; Hamersmark et al., 2008; Essaid and Hill., 2014), which would tend to decrease streamflow. We therefore focus the remaining modelling on summer-time valley-floor drainage, to which any increased streamflow might be attributed.

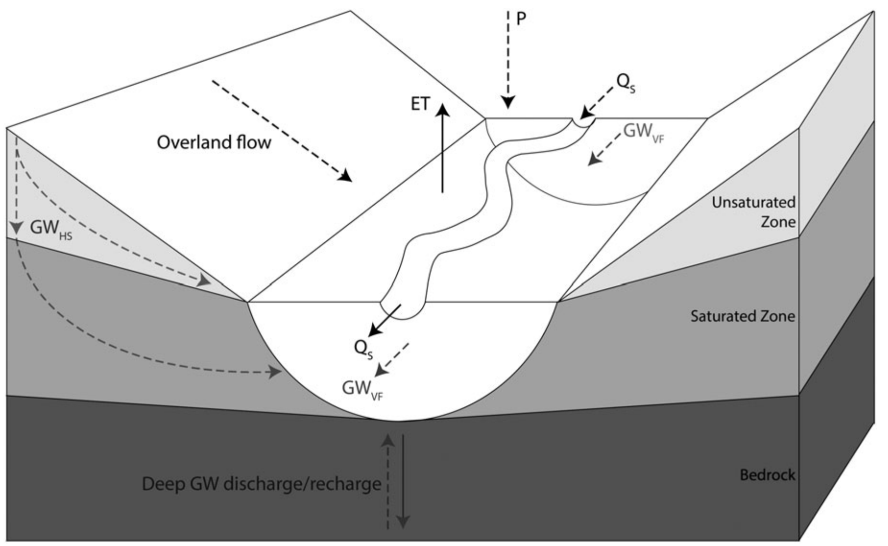

FIGURE 1 Schematic representing water fluxes into and out of an upland valley floor (meadow). Abbreviations as described in text. We assume that the changes to deep GW (groundwater) and overland flow as the result of restoration are negligible. After Essaid & Hill, 2014

2.2 | A physically based model for valley floor contributions to streamflow

To determine the volume of streamflow that can be attributed to changes in valley storage as a result of meadow restoration, we developed a model to calculate: (a) the maximum storage physically available in a given valley, (b) the fraction of that storage available for gravity-driven drainage to a channel, and (c) the temporal pattern of drainage based on the Boussinesq equation to calculate volume and timing of discharge to the channel. These drainage results are put into a hydrological context through comparison with estimates of groundwater contributions and evapotranspirative losses.

The total volume of water that can be stored in a valley is a function of its dimensions and the porosity of its fill material; the volume actually stored (V_{max}) is determined by the shallowest depth of the water table reaches annually (WTD_{min}). This can be represented as

$$V_{max} = 2BLn(D_z - WTD_{min}), \tag{6}$$

where B (L) is floodplain width on one side of the stream, D_z (L) is depth to bedrock, WTD (L) is the depth to the water table, L (L) is meadow length, and n (L_3 /L_3) is porosity; the dimensions are multiplied by 2 to account for volume changes on both sides of the stream (Figure 2a). As the water table drops to its maximum depth, only a fraction of the total stored water will drain—the rest will be held in pores by capillarity and other physical forces. We must then define the drainable porosity, φ, as the volume of water that will drain from an area per unit drop in water table (Bear, 1972; Brutsaert, 2005). Integrating this over the valley area gives our drainable storage (volumetric yield; V_W):

$$V_W = V_{max}\frac{\varphi}{n} = 2BL\varphi(D_z - WTD_{min}). \tag{7}$$

This formulation assumes that the water table is constant across the entire floodplain, though it is common for the depth to water table to increase nearer the channel, particularly in meadows where incision has proceeded nearly to bedrock (Loheide & Gorelick, 2007). The assumption that the water table is constant as a starting condition serves both to simplify the initial conditions and maximize expected changes in groundwater storage, both of which are goals of this modelling exercise. As water can only drain into an open stream via gravity, we note that only water held above the channel surface elevation can drain laterally into the channel, or: that the water in a valley that drains into the local channel is coming from the two blocks of fill immediately adjacent to the channel (Figure 2b). The remaining water is available for longitudinal drainage, which is groundwater that flows down valley through valley fill. This water will eventually discharge either on the valley surface or within the channel when the land surface intersects the potentiomatic surface, though it also commonly directly feeds ET and may never discharge (Essaid & Hill, 2014; Lowry & Loheide, 2010). The amount of drainable storage available for lateral drainage (V_{lat}) is

$$V_{lat} = 2BL\varphi(D_i - WTD_{min}). \tag{8}$$

D_i (L) represents the depth of incision (ref Figure 2) .

The total volume that will drain until some time of interest (t_c) can be well approximated using the conservation of mass and Darcy's law under the Dupuit hydraulic flow assumptions (only horizontal flow and no recharge) embodied in the Boussinesq equation for the transient drainage of an initially saturated unconfined aquifer to a fully penetrating channel. This assumption requires that we adjust our representation of this meadow from the more realistic case where the channel only partially penetrates the valley fill (Figure 2a) to one where the channel has incised to bedrock (Figure 2b). This second representation provides a useful visualization of the volume of laterally drainable volume. In this well-established approach (e.g., Brutsaert & Nieber, 1977; Rupp et al., 2004) the changing elevation of the water table a distance x from the stream in the floodplains adjacent to the channel are represented by

$$\frac{\partial h}{\partial t} = \frac{K}{\varphi}\frac{\partial}{\partial x}\left(h\frac{\partial h}{\partial x}\right), \tag{9}$$

where h (L) is the elevation of the water table, t (t, days here) is the time since the start of recession, and K (L/t) is hydraulic conductivity. Homogenous valley fill extends from an impermeable bedrock layer at z = 0 to the valley floor surface at z = D_i (Figure 2b). This can be analytically solved either for an early-time solution, where drainage occurs only from fill adjacent to the channel and has not yet reached the valley floor edge (x = t_1 in Figure 2), or for late time when the water table is lowering along its entire width (x = t_2 in Figure 2; Rupp & Selker, 2005). Since we are interested in late-summer streamflow following spring snowmelt (t_c~100 days after the start of drainage), it is appropriate to assume a late-time solution, and its associated boundary conditions, when it is assumed that the surface of the water table will resemble an inverse, incomplete beta function

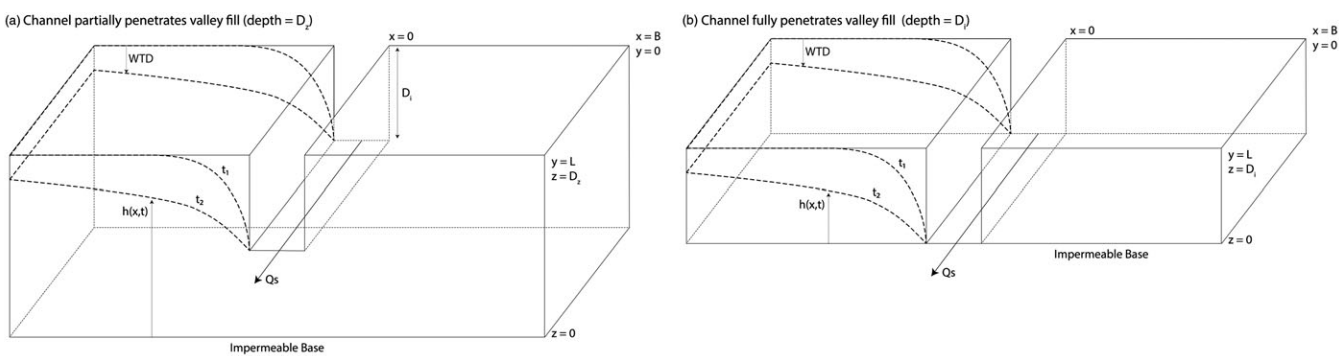

FIGURE 2 Dimensional sketch of upland valley floor, channel, and time-variable water table position for any unimpeded channel cut into valley fill. After Rupp and Selker (2005)

(Brutsaert & Nieber, 1977). To facilitate the development of an analytical solution while maintaining accuracy through the bulk of the drainage process, we employ the standard linearization of the equation by approximating the thickness through which the water flows as the average water table depth (h = [D_i–WTD]/2 in Equation 9; Brutsaert, 2005). Linearization assumes that the aquifer thickness is much greater than the change in water table elevation, which may not always hold for meadow aquifers. Rearranging terms with the linearized water table depth produces

$$\frac{\partial h}{\partial t} = \frac{KD_i}{2\varphi}\frac{\partial^2 h}{\partial x^2}, \tag{10}$$

subject to the boundary and initial conditions:

$$\begin{gathered} h(x=0,t)=0 \\ \frac{\partial h}{\partial t}(x=B,t)=0 \\ h(x=B,\ t=0)=D_i \end{gathered} .$$

The late-time solution separates space and time (e.g. h(x,t) = X(x)T(t))), each of which can be solved with respect to the given boundary and initial conditions, per Brutsaert and Nieber (1977), and recombined to give

$$h(x,t) = D_i \sin\left(\frac{\pi}{2B}x\right)e^{-\frac{KD_i\pi^2}{8\varphi B^2}t}, \tag{11}$$

which indicates that the water table maintains a constant sinusoidal shape that decreases in amplitude exponentially with time since start of drainage. If the draining floodplains are not initially saturated, D_i must be adjusted to reflect the expected maximum elevation of the water table above the channel bed (e.g., in an incised channel 3 m deep with a water table 1 m beneath the valley surface, D_i = 2 m).

We can improve our approximation of the laterally drainable subsurface storage (V^*_{lat}) using Equation 11, by calculating the differences between the modeled water table surfaces at the start of drainage (t_1) and our time of interest (t_c).

$$V^*_{lat} = 2\varphi L \int_0^B [h(x,t_1) - h(x,t_c)]dx. \tag{12}$$

This formulation assumes that there are no inputs and that the only system output is valley fill drainage to a channel. Valley floors are, however, also typically losing water to evapotranspiration or receiving groundwater from the surrounding landscape (upstream valleys and hillslopes, refer to Figure 1). Including the effects of a net loss or gain due to groundwater upwelling and evapotranspirative consumption is essential in estimating the water table position and water budget. The linearization of Boussinesq ($h = D_i/2$ in Equation 10) is central to this, as it allows us to superimpose an additional solution for a system experiencing changes in storage. Looking to the nonstreamflow-related inputs and outputs, we compute the change in storage as

$$\varphi\frac{dh}{dt} = GW_{HS} - ET_G, \tag{13}$$

where GW_{HS} (L/t, here m/day) represents the groundwater inflow from surrounding hillslopes and up-valley locations and ET_G (L/t, here m/day) represents the rate of evapotranspiration from groundwater. These seasonally averaged values can be calculated by closely analysing the diurnal fluctuations in WTD. Specifically, as suggested by White (1932), we attribute reductions in water table depth at night to groundwater influx to a valley bottom and increases during the day to plant and evaporative use in excess of groundwater contributions. Per the formulation of White's method presented by Lautz (2007)

$$ET_G = \varphi(24r_{gw} + \Delta s), \tag{14}$$

$$GW_{HS} = 24\varphi r_{gw}, \tag{15}$$

where r_{gw} (L/t, here m/hr) is the rate of water-table rise between 0:00 and 4:00, and s (L, here m per Lautz, 2007) is the net rise or fall of water table during a 24-hr period. This approach assumes hillslope groundwater inflow is constant, that the lowering water table is due to evapotranspiration, and that evapotranspiration and soil-water hysteresis are small in the predawn period (Loheide & Gorelick, 2005; White, 1932). The assumption of GW as constant may not necessarily hold, as the vegetated hillslopes will experience their own diel ET cycles that would propogate into the meadow. More specific discussion of the conditions under which diel fluctuations occur can be found in Loheide and Gorelick (2008).

Substituting the values from Equation 14 and 15 into Equation 13 accounts for changes in the depth to water table due to groundwater inflow and evapotranspiration at a daily timescale, and explicitly solves for the water table position's rate of change. Integrating this with respect to time solves for the total change in water table height:

$$h(t) = \frac{GW_{HS} - ET_G}{\varphi}t = \Delta st. \tag{16}$$

This solution can be superimposed onto Equation 11 to model the time evolution of the water-table height and obtain an overall model for the meadow water-table dynamics:

$$h(x,t) = D_i \sin\left(\frac{\pi}{2B}x\right)e^{-\frac{KD\pi^2}{8\varphi B^2}t} + \frac{GW_{HS} - ET_G}{\varphi}t. \tag{17}$$

The addition of the second term refines our estimate of the position of the water table and the total volume of water drained between t_1 and t_c. Given the no-flux boundary conditions, however, the results will not accurately represent the spatial distribution of the upwelling

TABLE 1 Dimensions of modeled upland valley floor

Parameter		Value
Floodplain width	B	200 m
Channel width	B_c	6 m
Depth to bedrock	D_z	10 m
Reach length	L	1,000 m
Volume of meadow fill		4,000,000 m^3
Longitudinal gradient	S	0.01 m/m
Depth of incision	D_i	"Restored": 0.33 m Incised: 1 m Deeply incised: 3 m
Soil media		Silt loam
Porosity	n	0.45
Drainable porosity	ϕ	0.1
Hydraulic conductivity	K	0.5 m/day

groundwater, as will be seen when compared with field data. To explicitly calculate drainage rate on a given date, we integrate Equation 17 spatially over the meadow area, multiply by the drainable volume of water per change in water table height, and take the time derivative to obtain the predicted rate of change of stored water. Per Brutsaert and Nieber (1977), the long-time solution to the linearized Boussinesq equation can be reduced into an exponential decay equation:

$$Q(t) = V^{*}_{lat}\,\alpha e^{-\alpha t}, \tag{18}$$

where V^{*}_{lat} is total lateral drainage calculated in Equation 12 for t_1, and α is a decay constant that describes the physical properties of the system. Discharge values produced by this equation are maximized by setting α equal to one over the square root of t_c, which assumes that the chosen valley has optimal physical conditions for producing streamflow at t_c.

Having established the lateral drainage volumes and rates, we next address the question of longitudinal drainage through the valley floor. Realistically, drainage will occur in three dimensions, the dominant vector of which will be along the largest available hydraulic gradient. The magnitude and direction of the maximum hydraulic gradient is a function of down-valley and cross-valley gradient, soil media, and the seasonally variable position of the water table relative to the water surface elevation in the channel (Barry, Parlange, Sander, & Sivaplan, 1993; Loheide & Gorelick, 2007; Richards, 1931). To estimate the relative contributions of lateral and longitudinal drainage to streamflow, we assume all water is draining along the largest available hydraulic gradient towards the base of the channel at the downstream end of the valley (x, y, z; = 0, L, 0; Figure 2b). For lateral drainage, we assume an average initial position at (B/2, 0, and D_z); for longitudinal drainage, we assume an average initial position at (B/2, L, and D_i) (Figure 2b). These initial positions represent the maximum width-averaged hydraulic gradient available, which maximizes our drainage volume estimates within the bounds of realistic conditions. We assume drainage occurs across the maximum available cross-sectional area which, for lateral flow, includes the entirety of both stream bank faces along the entire reach; for longitudinal flow, this is the cross section of the upland valley extending to bedrock. Reformulating Darcy's law to include the geometric values for these two scenarios, we predict maximum flow rates as

$$Q_{lat} = 4KL\frac{D_i^2}{B}, \tag{19}$$

$$Q_{long} = 2KBD_i\frac{LS + D_i}{\sqrt{\frac{B^2}{4} + L^2}}, \tag{20}$$

where S (L/L) represents longitudinal valley slope. Assuming equivalent saturated hydraulic conductivity and valley dimensions, we can solve for the dominant direction of flow in any given scenario. Comparing the solution to Equation 19 with the t_1 solution for Equation 18 provides a scale by which to evaluate the magnitude of the solution to Equation 20 in the context of expected discharge. This gives a first-order estimate of how changing the channel depth through restoration will affect dominant flow paths, and places upper bounds on expected streamflow contributions from both lateral and longitudinal drainage. Secondarily, these formulations—being entirely geometric—allow us to compare geomorphic conditions and thresholds in upland valleys that influence the dominant flow path.

2.3 | Selecting model parameters to maximize expected change in streamflow following restoration

Selecting model parameters requires balancing the goal of maximizing conditions for the production of late-season water and accurately representing the typical conditions encountered in upland valley floors. We recognize that there is considerable variation in upland valley systems, and have adopted parameters that provide an upper limit on the potential changes in storage and contributions to flow based on our geologic understanding of hydraulic parameters in these systems; our calculations are therefore biased in favour of the largest potential hydrologic impact of restoration (Table 1).

Soil media was selected from the range of typical soils found in upland valley fill both from field investigations and literature reported values (Birkeland & Janda, 1971; Koehler & Anderson, 1994; Walter & Merritts, 2008; Wood, 1975). Silt loam was specifically selected for balancing the trade-offs between high-porosity and high-hydraulic conductivity. The values for those properties listed in Table 1 were selected from the upper end of associated ranges.

To assess the sensitivity of flow to depth of incision and the magnitude of change in flow relative to initial conditions, we model three scenarios: a channel that is 3 m deep (C-3), 1 m deep (C-1), and 0.33 m deep (C-0.33). These are common depths of incision in upland valley floors, though are certainly small compared with some extreme examples (>20 m; Antevs, 1952; Bull, 1997; Harvey & Watson, 1986; Peacock, 1994; Simon, Curini, Darby, & Langendoen, 2000). We exclude those large depths as they would be unlikely candidates for the styles of restoration being examined here.

The minimum meadow water table depth (WTD_{min}) will vary considerably on the basis of the climate, including spatiotemporal patterns of snowmelt (Lowry et al., 2010), soil media properties (Loheide et al., 2009; Essaid & Hill, 2014), and stream stage (Lowry et al., 2010) in the meadow. For the purposes of this modelling exercise, we are interested in capturing the largest expected change in water-table depth, so as to maximize changes to groundwater storage. Loheide and Gorelick's (2007) model hydrographs show a difference in WTD_{min} between restored and deeply (4 m) incised to be 0.75 m. Tague et al. (2008) reported a maximum change following restoration of 0.3–0.4 m. Hammersmark et al. (2008) report a maximum change of 1.2 m following restoration. Klein et al. (2007) reported no statistically significant changes following restoration. Based on these observed post-restoration changes in depth to the water table along incised channels of similar magnitude, we set WTD_{min} as 1 m in C-3, 0.3 m in C-1, and 0 m(e.g., saturated valley fill) in C-0.33, which effectively represents a 1 m change in $\mathrm{WTD}_{\mathrm{min}}$ following restoration. These values represent the upper bounds of expected change to WTD_{min} as presented in the literature and more importantly, represent a general trend of decreasing WTD_{min} with decreasing incision that is relatively consistent across study sites.

The day of year we chose to represent the start of drainage (t_1) was based on data from piezometers installed along existing, incised (1 m) meadows on the Middle Fork John Day (MFJD, Figure 3), which shows that the water table begins to draw down (t_1) on June 10 (Figure 5). This value can easily be adjusted based on local climate, and is not a primary control on the pattern of drainage volume outputs. As we are interested

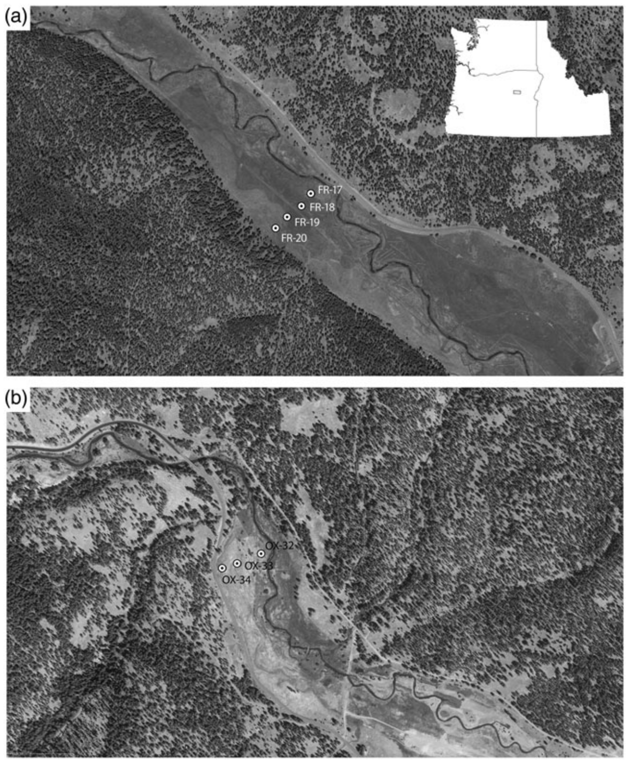

FIGURE 3 The study site for meadow drainage on the Middle Fork of the John Day River (a) with an example of a 4-well transect in the Forrest property which is immediately downstream of Bates Oregon, and 15 km upstream of the (b) similar 3-well transect at Oxbow. The site is located in northeastern Oregon, USA

in changes to late-summer streamflow, we selected an index date of September 1 on which to evaluate changes in streamflow following restoration (t_c = 82 days following start of drainage). Modelled results from Loheide and Gorelick (2007) indicate that a reduction in depth of incision should result in an extended duration of WTE_{max}, as streamflow levels are kept higher in a smaller channel. Per the diminishing exponential relationship between valley floor discharge and elapsed time (Equation 18), a t_c nearer to t_1 should result in a larger daily streamflow contribution on the index date. We therefore extend t_c to reflect an earlier start of drainage in the most deeply incised scenario (t_c = 92 days in C-3) and reduce t_c for the least incised, or "restored" scenario (t_c = 77 days in C-0.33). The reduced t_c value in the least incised, or "restored" scenario (C-0.33) increases the potential contributions of bank storage to streamflow on the selected index date.

2.4 | Testing model assumptions against field data from meadows on the Middle Fork John Day River, Oregon.

We test the validity of assumptions made in our model by comparing modeled water tables to water tables measured in two floodplain meadows along the MFJD River, Oregon (Figure 3). We use the dimensions of the floodplain at each site to calculate change in WTD due to drainage and the diurnal signal in two well transects to estimate net effect of groundwater upwelling and evapotranspiration to produce modelled water table surfaces (Equation 17, Figure 5). This gives an estimate of the total volume drained over the summer and temporally explicit drainage rates, or meadow contribution to streamflow.

The MFJD flows for 120 km, draining 2,100 km^2 of the Blue Mountains in Northeastern Oregon, USA. The watershed receives 380–640 mm of precipitation annually, the majority of which occurs between October and June as snow. The channel is, on average, 1 m deep and 4 m wide; average streamflow is 7 m^3/s, with peak streamflow of 22.7 m^3/s occurring in midspring. Mean daily streamflow at t_1 (June 10) is 12.1 m^3/s and decreases to 0.9 m^3/s at t_c (September 1). The soils in the floodplains are mostly clay loam (Noël, unpublished data) which have a drainable porosity of roughly 0.02 (Loheide & Gorelick, 2005). County-wide soil surveys estimate local hydraulic conductivity values ranging from 0.02 to 20 m/day (Dyksterhuis, 1981). Field tests at this site suggest that 5 m/day is an appropriate magnitude for soils in the area of the well transects (Noël, unpublished data). The Forrest transect is composed of four wells spaced evenly between 50 and 240 m laterally from the channel (Figure 3a). The Oxbow transect is composed of three wells evenly spaced between 50 and 200 m laterally from the channel (Figure 3b). Water table elevation was collected continuously at both sites from 2009 to 2010.

The annual hydrograph of each floodplain meadow shows that the water table was maintained within 0.3 to 0.8 m of the surface throughout the year (Figure 4a). Minimum WTD (0.3 m) occurred in early June, so we set June 10, 2010 as the start of drainage (t_0), which is consistent with values reported elsewhere (Hammersmark et al., 2008; Klein et al., 2007; Loheide & Gorelick, 2007; Tague et al., 2008). Despite several large summer storms (e.g., July 26, 2010, and August 11, 2010), there was no detectable response in WTD during summer drawdown (Figure 4b).

Diurnal fluctuations in the water table are the result of the combined effects of drainage, groundwater upwelling, and evapotranspiration (Figure 4b). Minimum daily WTD occurs around 0700 and lowers to its maximum daily depth around 1700. The daily decrease can be attributed to evapotranspirative losses exceeding groundwater upwelling.

We can estimate average daily GW_{HS} contributions and ET_G losses using EQN 14 and 15. We calculate values for July, when peak ET is expected to occur in meadow systems (Hammersmark et al., 2008; Table 2). Predicted values for both ET_g and GW_{HS} are consistent between sites. The values for ET_g are lower than literature reported values for ET in native meadows, which range from 5 to 7 mm/day (Hammersmark et al., 2008; Loheide & Gorelick, 2005). This is likely due, in part, to the predicted ET dilution as a result of diel fluctuations in the GW_{HS} input that are not explicitly accounted for by this formulation. Since potential ET at this site in July is over 9 mm/d (BATO Station data available at https://www.usbr.gov/pn/agrimet/monthlyet.html), the low rate of consumption by plants may also reflect the limitations of the combined stored water and groundwater available. Had more water been available, for instance, if a restoration project had elevated the water table, these rates would be expected to increase towards the upper limit of PET (Lowry & Loheide, 2010).

The volume of water lost daily through evapotranspiration is consistently larger than the net volumetric contribution from groundwater inflow (310 mm per unit valley width) (Table 3). We tested the validity of using an averaged rate of evapotranspiration by comparing the total observed change in WTD in July 2010 with predicted change using the average value. Between July 1 and 31, the WTD

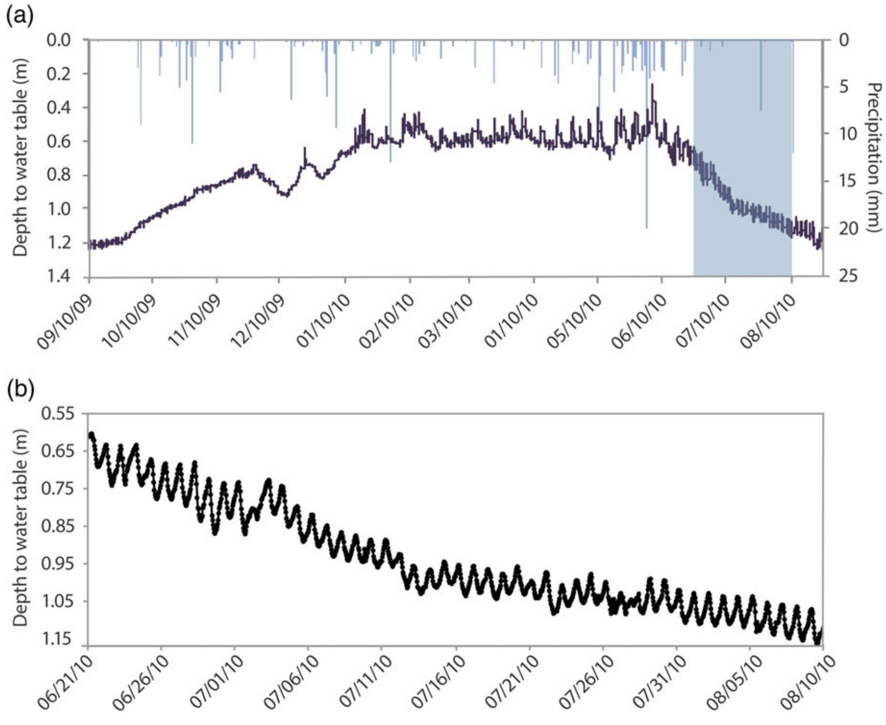

FIGURE 4 (a) Depth to water table at Oxbow-34 during 2009 water year. Precipitation shown on top of graph is from Agrimet station in Prairie City, 25 km to the south. (b) Daily signal in water table elevation during the decrease of the water-table at Oxbow well 34 during portion of summer of 2010 (shaded in [a])

TABLE 2 Calculated ET_g and GW rates for all wells at both sites for July 2010

	Forrest 17	Forrest 18	Forrest 19	Forrest 20	Oxbow 32	Oxbow 33	Oxbow 34
ET_G (mm/day)	2.4	2.7	2.2	1.8	2.1	2.6	2.7
24^*r_{GW} (mm/day)	106	115	85	77	94	117	123
GW_{HS} (mm/day)	2.1	2.3	1.7	1.5	1.9	2.3	2.5

in Forrest-19 dropped 720 mm Predicted change in WTD using the averaged ET rate was 770 mm, an error of 50 mm (7%). The uncertainty associated with other parameters used in Equation 11 (e.g., hydraulic conductivity and drainable porosity) can often range over two orders of magnitude for a given site, and thus, the much smaller error associated with using averaged ET is considered acceptable for this application.

To assess temporal variation in prediction error, we modelled the water table elevations for both sites on the first day of each month from May through August using parameters given in Table 3 (Figure 5). The average error between modelled and observed water table surfaces on all dates was 50 mm for Forrest and 49 mm for Oxbow (Table 4)—a 5.2% and 5.4% error from mean depth to water table over the period of interest, respectively. The average monthly error was

TABLE 3 Model inputs and results for Forrest and Oxbow sites at Middle Fork John Day, OR

			Forrest	Oxbow
Channel depth	D_i	m	1.6	1.12
Time of interest	t_c	days	51	51
Max WTE, below valley floor	WTE_{max}	m	0.3	0.3
Valley width	B	m	240	200
Drainable porosity	ϕ	m^3/m^3	0.04	0.04
Hydraulic conductivity	K	m/day	5.87	5.45
Laterally drainable storage per km	V_{lat}	m^3	62,400	32,800
Volume drained per km, t_0 to t_c	V_{lat}^*	m^3	4,180	2,460
Max lateral discharge	Q_{lat}	m^3/s	2.9×10^{-3}	1.6×10^{-3}
Max longitudinal discharge	Q_{long}	m^3/s	9.5×10^{-4}	7.0×10^{-4}
Discharge per km, $t = t_c$	$Q\text{-}t_c$	m^3/s	6.0×10^{-5}	3.3×10^{-5}
Discharge per km, $t = t_1$	$Q\text{-}t_1$	m^3/s	6.6×10^{-2}	3.6×10^{-2}
Total discharge per km, $t = t_c$	$Q_{tot}\text{-}t_c$	m^3	5.2	2.8
Total discharge per km, $t = t_1$	$Q_{tot}\text{-}t_1$	m^3	5,700	3,100

Note. The index date for these model runs was set to August 1, hence the smaller t_c values.

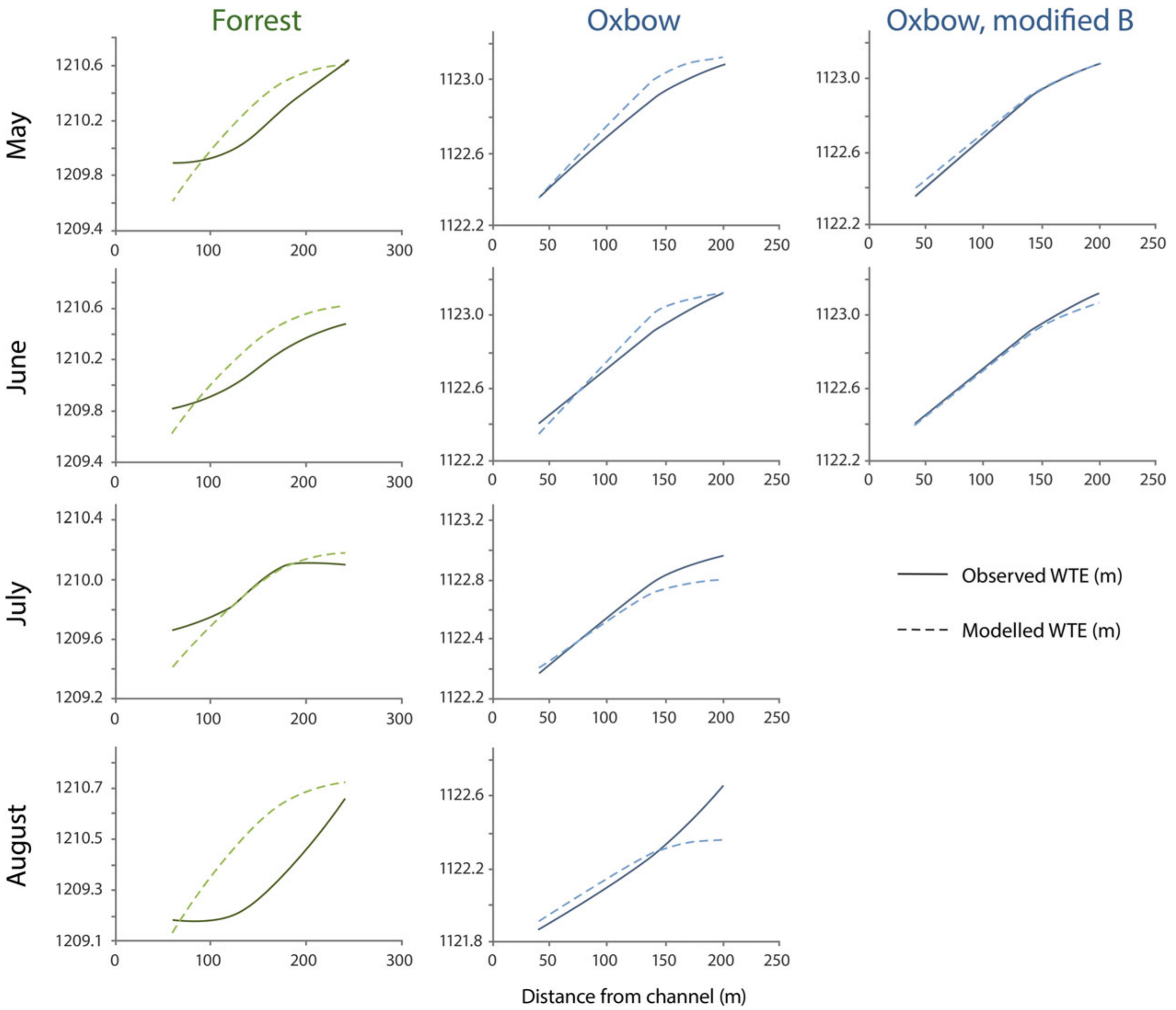

FIGURE 5 Observed (solid line) and modeled (dashed line) water table surfaces at Forrest and Oxbow sites, May 1 to August 1, 2010. Modifying valley width to be slightly larger at the Oxbow site improves the fit of early season calculated water table surfaces

TABLE 4 Average error between calculated and observed water table surfaces at Forrest and Oxbow sites from May to August 2010

	May 1, 2010	June 1, 2010	July 1, 2010	August 1, 2010	Site average, mm
Forrest (mm)	24	77	39	70	50.25
Oxbow (mm)	42	09	67	78	49
Monthly Average (mm)	33	43	48.5	74	49.6

smallest in May (33 mm) increasing to maximum error in August (74 mm), with errors of 5.5% and 6.1% from mean depth to water table at each site, respectively. The observed results at Oxbow closely fit the magnitude of change predicted by the model. The congruence between observed and predicted curves is less as the Forrest site, but the model still predicts the overall trend rather well for all months except August. Model fit was improved by extending the floodplain width 50 m beyond the well furthest from the channel (B = 250 m) (Figure 5). Neither site accurately captures the shape of the observed water table, which is considerably higher at the meadow margins and lower at the channel edge than predicted. This is due to the no-flux boundary condition imposed on this model, which while necessary for the simplification, does not capture GW inputs to the meadows from adjacent hillslopes throughout the summer. In general, observed elevations are lower than calculated values, which is consistent with our goal of maximizing expected changes to groundwater storage.

The volume of flow draining from the meadow to the river can be computed using this model. For the index date of September 1, the drainage from meadow to the stream at Forrest was 6.0 × 10^{-5} m^3/s/km of stream and at Oxbow was 3.3 × 10^{-5} m^3/s/km (an increase in stream flow of between 33 and 60 ml/s/km of meadow adjacent to the stream). Given this river had a mean daily flow on September 1 of about 0.9 m^3/s, this represents less than 0.01% flow contribution per kilometre, which is considerably lower than typical measurement errors for standard stream gauging techniques (e.g., Sauer & Meyer, 1992) suggesting that any flow contributions from the meadow would be undetectable. To put the contributions of lateral inflow to streamflow in context, if we were to assume this rate of inflow occurred over the entire length of the MFJD River, the total contribution would be 7.2×10^{-3} m^3/s or about 0.8% of the mean daily September 1 flow. The maximum longitudinal flow (Equation 20) predicted for this site was an order of magnitude smaller than the maximum lateral flow (Equation 19), indicating that longitudinal flow should account for an even smaller percentage of mean daily September 1 flow. This result is consistent with the fact that the total change in volume of water stored in the meadow is insignificant compared with seasonal stream flow, as we will show in the next section of this paper.

3 | RESULTS AND DISCUSSION

To explore the upper physical bounds on potential streamflow contributions due to restoration, we modelled three incision-depth scenarios (C-3, C-1, and C-0.33) using a set of parameters selected to maximize potential streamflow contributions (Table 1). The results from our model and field tests suggest that wet-meadow restoration is not likely to result in significant increases in late-summer streamflow and may actually decrease flows given the likelihood of increased evapotranspirative use as the water tables in the meadow is raised into the root zone.

3.1 | Total storage increases with restoration but laterally drainable storage decreases

Though reduced incision is associated with increased total storage, less of that storage is accessible for lateral drainage to the channel. Total storage increases from 1.6×10^6 m^3 in the deeply incised channel (C-3) to 1.8×10^6 m^3 in the least incised channel (C-0.33)—an 11% increase, due in large part to less incised channels having shallower water tables. However, the laterally drainable storage in the least incised channel (C-0.33) decreases by an order of magnitude—from 14,150 to 330 m^3 or roughly 98%—when compared with a deeply incised channel (C-3) (Figure 6). This is due largely to the reduced hydraulic gradient along which water drains to a less incised channel, and the smaller drainage face through which drainage reaches the channel.

The volumes of total storage (V_{max}) and drainable storage (V_W) are inversely proportional to the depth of incision; deeper channels typically have lower maximum water table elevations (WTE_{max}) and therefore store less water. The increase in storage is therefore a function of the imposed values of WTE_{max}, which were selected from literature values to produce a best-case scenario for changes to storage and drainage. For instance, WTE_{max} selected for the least incised, or "restored" scenario (C-0.33) was set at 0 m, despite field data typically indicating that maximum water table elevations fall 0.7–1.3 m below the surface (Klein et al., 2007; Loheide & Gorelick, 2007; Hammersmark, 2008; Tague et al., 2008). This overestimation increases confidence in the trends demonstrated by the analysis, and while the absolute volumes are a function of imposed valley dimensions and soil media properties, the direction of change should hold for any scenario.

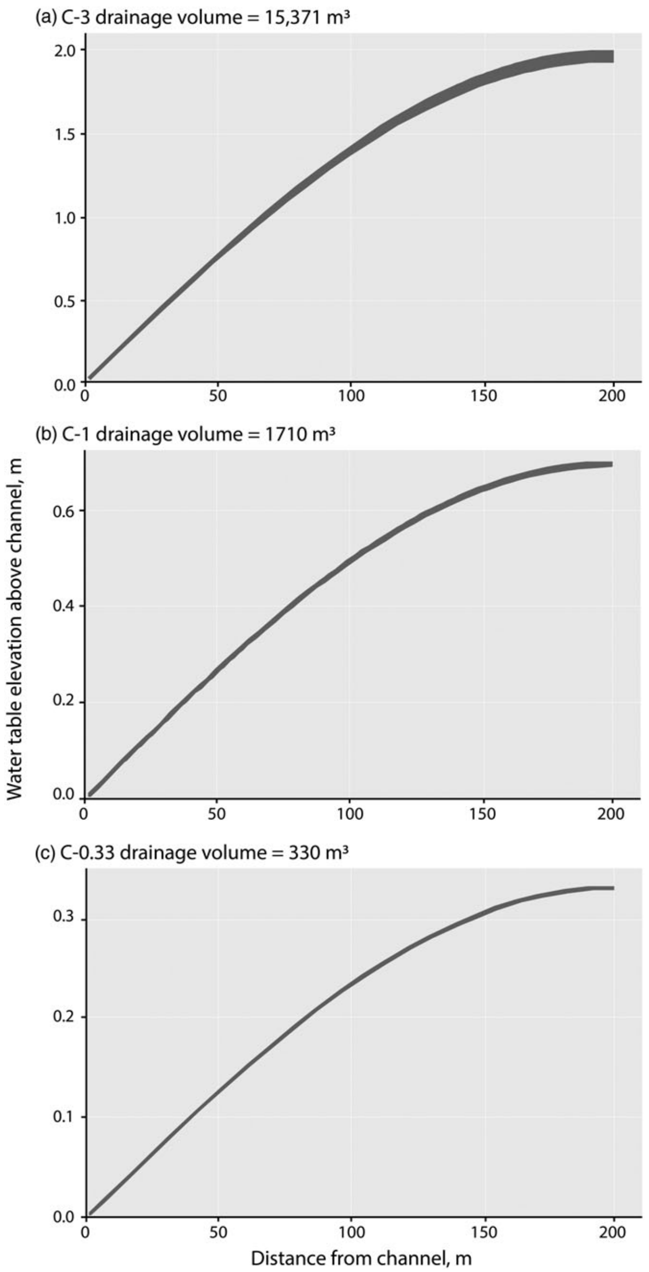

FIGURE 6 Drainage curves produced from Equation 12 for (a) 3-m incised scenario (C-3), (b) 1-m incised scenario (C-1), and (c) 0.33 m incised or "restored" scenario (C-0.33). Top of the curve shows position of water table at t_1, bottom of curve shows position of water table at t_c. Note differences in scale of Y axis and considerable vertical exaggeration

3.2 | Evapotranspirative use increases in restored meadows

Though not directly modelled by this exercise, empirical data and modelled results demonstrate that increasing the elevation of water table into the root zone increases evapotranspirative use both by reducing water stress in existing vegetation and shifting communities towards denser, more mesic species (Hammersmark et al., 2008; Hammersmark et al., 2009; Loheide, 2008; Loheide & Gorelick, 2005; Loheide & Gorelick, 2007). Published data indicate that this shift from xeric to mesic or hydric vegetation typically increases evapotranspirative demand by between 1.5 and 3 mm/day (Hammersmark et al., 2008; Loheide & Gorelick, 2005; Loheide & Gorelick, 2007). Over the surface area of the modelled meadow (Table 2), the minimum predicted ET shift would increase water usage by 600 m^3/day throughout the summer or by 48,000 m^3 over the drainage period of interest. Whether due to reduced water stress or new species with higher evapotranspirative usage, restored meadows should be expected to have higher ET than unrestored meadows, making the solution to ($ET^U - ET^R$) negative.

3.3 | Streamflow decreases in restored meadows

Increased ET and reduced drainable storage in restored meadows is predicted to lead to an overall decrease in valley discharge ($\Delta Q_{V,\ out}$). The volume of water drained in the deeply incised scenario (C-3) is larger than the volume drained in the least incised, or "restored" scenario (C-0.33), making the solution to ($\Delta S^U - \Delta S^R$) negative (Equation 5). This result, coupled an increase in evapotranspirative demand following restoration, gives strong evidence that valley discharge should decline following restoration. Though restoration increases the total amount of water stored in meadows, the new storage does not discharge to streamflow. The majority of this new storage is, instead, likely used to support a higher evapotranspirative demand from previously water-stressed plant communities or denser, mesic-plant communities. That said, even if ET were neglected, the changes in the geometry of a restored system also tend to decrease streamflow by reducing hydraulic gradients along which groundwater discharges.

Modelled results demonstrate both a reduction in streamflow and that valley discharge contributes very small volumes of water to streamflow in any scenario. The rate at which stored water drains laterally to the channel decreases both in early and late time in the restored scenario (Table 5). On the selected index date, September 1, the model predicts that a kilometre of deeply incised channel (C-3) will drain 1.2×10^{-6} m^3/s to streamflow; a kilometre of restored valley (C-0.33) storage will drain 7×10^{-8} m^3/s. Both values represent less than 0.01% of an average daily flow rate of 0.1 m^3/s. Moreover, the restored valley will contribute two orders of magnitude less streamflow than the incised valley.

On the first day of drainage (t_0 = June 11), 1 km of deeply incised valley (C-3) is predicted to contribute 1330 m^3/km to streamflow; 1 km of restored valley (C-0.33) contributes a total of 33 m^3. This amounts to average flow rates of 1.5×10^{-2} and 3.8×10^{-4} m^3/s, respectively, per kilometre of stream. However, drainage this early in the season is more likely to fall under the assumptions of short-time drainage, and the modeling employed here is likely inappropriate for estimating anything other than relative magnitudes of early-season flow. The restored scenario, again, contributes less to the channel due to the reduced bank height and lower hydraulic gradient in the valley fill. This reduction in flow is consistent with modelled results demonstrating that peak flood flows downstream of a restored channel are reduced (Essaid & Hill, 2014; Hammersmark et al., 2009) and suggests the mechanism reducing peak flow into the channel is the same mechanism that lowers overall lateral drainage to the channel: reduced channel depth (hence drainable bank height) and decreased hydraulic gradient.

To account for potential streamflow augmentation downstream of the restoration site, we evaluated the upper bound on expected longitudinal contributions to streamflow using a geometric estimation of the maximum longitudinal hydraulic gradient. Previous modelled results suggest that restoration projects that reduce incision favour longitudinal discharge over lateral (Hammersmark et al., 2008; Loheide & Gorelick, 2007), which can be a favourable restoration outcome. To account for potential streamflow augmentation downstream of the restoration site, we evaluated the upper bound on expected longitudinal contributions to streamflow using a geometric estimation of the maximum longitudinal hydraulic gradient.

In all the modelled scenarios, as well as the field data, the maximum lateral flow rate calculated by the geometric method (Equation 19) is an order of magnitude greater than the peak lateral flow rate calculated by the more explicit linearized late time

TABLE 5 Model results for incised and restored scenarios, with percent change

			Deeply incised (C-3)	Incised (C-1)	% Change (C-3 to C-1)	Restored (C-0.33)	% Change (C-3 to C-0.33)
Channel depth	D_i	m	3	1	−66.7	0.33	−89.0
Time of interest	t_c	days	92	82	−10.0	77	−15.0
Max WTE, below valley floor	WTE_{max}	m	1	0.3	−70.0	0	−100
Available Storage	V	m^3	1,800,000	1,800,000	0.0	1,800,000	0.0
Maximum Storage	V_{max}	m^3	1,620,000	1,746,000	+7.8	1,800,000	+11.1
Drainable Storage	V_W	m^3	360,000	388,000	+7.8	400,000	+11.1
Laterally drainable storage per km	V_{lat}	m^3	80,000	28,000	−65.0	13,200	−83.5
Volume drained per km, t_0 to t_c	V_{lat}^*	m^3	14,146	1,558	−90.0	326	−97.7
Max lateral flow rate	Q_{lat}	m^3/s	1.0×10^{-3}	1.2×10^{-4}	−88.0	1.3×10^{-6}	−98.7
Max longitudinal flow rate	Q_{long}	m^3/s	3.0×10^{-4}	2.5×10^{-4}	−16.7	2.4×10^{-4}	−20.0
Discharge at t = t_c	$Q(t_c)$	m^3/s	1.2×10^{-6}	2.3×10^{-7}	−80.8	6.6×10^{-8}	−94.5
Discharge at t = t_1	$Q(t_1)$	m^3/s	1.5×10^{-2}	1.7×10^{-3}	−88.7	3.8×10^{-4}	−97.5
Total discharge, t = t_c	$Q_{tot}(t_c)$	m^3	1.0×10^{-1}	2.0×10^{-2}	−80.0	5.7×10^{-3}	−94.3
Total discharge, t = t_1	$Q_{tot}(t_1)$	m^3	1,329	154	−88.4	33	−97.5
Daily ET (from: Loheide & Gorelick, 2005)	ET	mm/d	3.0	5.0	+66.7	5.5	+83.3
Total ET usage, t = t_c	ET_{tc}	m^3	1.0×10^5	1.6×10^5	+49.1	1.7×10^5	+54.0

Boussinesq equation (Equation 18). This is to be expected, as the large, near-channel lateral gradients accounted for by the Boussinesq equation rapidly give way to lower overall hydraulic gradients in late time drainage.

Reducing channel incision shifts the dominant flow pathway from lateral to longitudinal, but the volumes of water discharged in both directions are smaller than in more deeply incised channels. In the more deeply incised scenario (C-3), maximum longitudinal flow rate is predicted to be an order of magnitude less than maximum lateral flow rate. Scaling by the lateral discharge calculated at t_c, we can expect longitudinal discharge at t_c to be a fraction of a mililiter per second. In the least incised, or "restored" scenario (C-0.33), maximum lateral flow rate decreases by an order of magnitude over the course of the drainage period, which is consistent with the change in discharge at t_c. Longitudinal flow rates do not appreciably decrease, indicating that a larger percentage of water stored in the restored scenario will drain longitudinally over the course of the drainage period, but the total contribution to flow is still negligible.

The scenarios modelled here optimize parameters towards streamflow generation; that the modelled volumes were very small in late summer for all scenarios indicates that drainage from low-gradient upland valley bottoms to their channels does not constitute a major source of late season streamflow. That the amount of streamflow draining from these features drops by orders of magnitude with reducing depths of incisions gives confidence that the pattern of reducing streamflow due to meadow restoration is correct.

3.4 | Alternative scenarios

The scenarios modelled in this analysis are of a straight channel through homogenous fill that extends down to bedrock. One benefit of a physically based, linearized model is the ease with which additional terms can be incorporated. In so doing, we can demonstrate that increasing sinuosity and adding a hydraulically conductive gravel lens do not appreciably increase the contributions of streamflow, and even if they do, the relative contribution still decreases with reduced incision (or restoration).

Lengthening the restored channel, either by increasing its sinuosity or adding a second braided channel, serves to increase the area from which the valley fill can drain and should theoretically increase drainage into the channel. If we increase the sinuosity of the restored channel from straight (sinuosity = 1.0) to meandering (s = 1.5) and add a second meandering channel with the same dimensions, we effectively triple the drainage face. This increases the volume of water drained over the day on September 1 (t_c) from 330 to 990 m^3. Though this is an overall increase in the contribution from the restored channel, the total volume is still two orders of magnitude less than the volume of water drained from the most deeply incised channel (C-3)—14,200 m^3.

This conclusion also stands if the analysis is expanded to consider a valley fill with a large, hydraulically conductive gravel lens (cross sectional area, $A = 1\ m^2$) continuous along the entire reach that acts as a preferential pathway (K = 90 m/day). Under these conditions, the valley could produce an additional 0.92 m^3/day ($1.1 \times 10^{-5}\ m^3/s$ of discharge) for a total discharge of $1.23 \times 10^{-5}\ m^3/s$. This discharge could potentially diminish over the course of the summer and could possibly be accessed by meadow or riparian vegetation, further reducing its storage and flux. Moreover, the general trend of decreased flow contributions with reduced incision would still hold.

3.5 | Physically based model results fit well with magnitude of change recorded in field data

The model accurately represented the magnitude of changes in water table elevations in two meadows over our period of interest (May–August). The goodness of fit decreases over the course of the summer, with modelled results underpredicting drainage from early-season floodplains, and overpredicting drainage from late-season floodplains. We remedied especially poor initial model fit by adjusting floodplain width in the model. The considerable differences in the modeled and observed shapes for the Forrest site may indicate a large groundwater input to this meadow from uplands.

The model's overprediction of late-season drainage serves the overall goal of conservatively modeling the maximum expected contributions of valley drainage to streamflow. This trend in error would correspond to the observed streamflows being higher than modelled results suggest in early season and lower than modelled results in late season. This overprediction of late-season streamflow serves the general purpose of the analysis by erring towards maximum possible streamflow in late season and gives an additional level of confidence in the observed trends.

Moreover, the relatively good fit of modelled results with field data bolsters confidence in the validity of combining the linearized long-time solution to the Boussinesq equation with estimates of evapotranspiration and groundwater upwelling using the White method and the utility of a physically based modelling effort in representing how changing geomorphic features affect hydrology.

3.6 | Theoretical strategies to maximize late-summer streamflow

Although our results demonstrate that even under the best of circumstances, increases in streamflow following wet meadow restoration are unlikely, the model highlights what manipulations and conditions would be necessary to theoretically increase streamflow. The maximum possible streamflow should occur when laterally drainable storage is large, and the time between start of drainage the time when streamflow is desired is small (Equation 18). Laterally drainable storage is optimized in long, fully saturated valleys with large depths of incision (effectively, large drainage face surface area; Equations 12 and 19). This is similar in principle to the practice of ditching or installing drainage tiles in fields or wet meadows where the goal is to drain stored water out of the fields. Critical time is minimized by extending the duration of maximum water table elevation, which can be accomplished by the persistence of surface floodplain storage or high in-channel water surface elevations that reduce lateral hydraulic gradients. Practically, this would be accomplished by saturating long reaches of upland valley, adding surface storage, maintaining a large surface area through which to drain the storage, and introducing a time-variable boundary condition at the channel edge or x = 0

(Figure 2). A time variable boundary condition might be introduced by lowering the water surface elevation in the open channel so that more laterally drainable storage is accessible as the summer progresses. These are, effectively, some of the hydraulic principles by which engineered dams increase late-season streamflow.

Geomorphic considerations include the dimensions and fill material of the valley in question. Per the geometric equations for maximum hydraulic gradient, lateral flow should dominate in long, gently sloping and narrow valleys; while longitudinal flow should dominate in short, steep, and wide valleys with limited to no channel expression. In both cases, valley fill with a high drainable porosity and hydraulic conductivity will increase floodplain contributions to channel discharge, though such fill often has lower overall porosity and storage capacity. If changes to streamflow are the only objective, maximum impact will be felt in places where vegetation is limited, or the vegetation communities will not likely change as a result of the restoration.

4 | CONCLUSIONS

Despite the implicit attraction of using wet-meadow restoration as a means of augmenting late-season streamflow, a physically based conceptual groundwater model employing reasonable assumptions of channel and valley hydraulic parameters suggests that no late-summer streamflow benefit should be expected by plug-and-pond styles of meadow restoration in most environments. While raising channel beds through restoration can increase total water storage in upland valley bottoms, the contributions of both lateral and longitudinal drainage from floodplains to late-summer streamflow are expected to decrease following wet-meadow restoration. Consistency in the magnitude of change between modelled results, field data, and previous research gives confidence that the basic model structure and assumptions are valid in their effort to represent maximum expected change.

Although regional late-summer streamflow increases should not be expected following wet-meadow restoration using plug-and-pond techniques, the demonstrated improvements in the quality and health of wetland vegetation could warrant considering such measures, even at the cost of increased evapotranspirative use. Increased evapotranspirative usage represents a change in either ecosystem type, or a reduction in water limitation—either of which might represent a valuable restoration objective. It is critical, however, to separate the achievable goals of improving ecosystem health and sustaining wetland ecosystems from the untenable goal of increasing late-season streamflow. Goal setting is a critical component of restoration projects, and the accurate representation of expected changes as a result of restoration is necessary for sustaining public trust and achieving desired outcomes. Without an understanding of the possible range of ecohydrologic responses to restoration, it is difficult to set reasonable metrics of success. The model presented here, and its initial results, can be used to set more realistic objectives for restoration programs, and help guide future research on how site-specific factors will affect the desired outcomes.

Future research can work to both expand this model's capacity in a range of other, geologically distinct environments and expand the application of this modelling approach to other restoration styles. For instance, artificial structures used in beaver-related restoration (e.g., beaver dam analogs, artificial beaver dams, etc.) often have similar goals as wet-meadow restoration (Pilliod et al., 2018) and the evaluation of such structures using this modelling framework would allow for a more realistic estimation of expected changes following restoration.

ACKNOWLEDGEMENTS

This work was funded by the U.S. Department of Agriculture Northwest Climate Hub and the U.S. Department of the Interior Northwest Climate Science Center. We thank four anonymous reviewers for the time and effort they provided to offer thoughtful input that improved both our thinking on the topic and this paper.

ORCID

Caroline S. Nash http://orcid.org/0000-0002-0339-619X
John S. Selker http://orcid.org/0000-0001-9751-6094
Sarah L. Lewis http://orcid.org/0000-0002-1824-8739

REFERENCES

Abbe, T., & Brooks, A. (2013). Geomorphic, Engineering, and Ecological Considerations when using wood in river restoration, stream restoration in dynamic fluvial systems. *American Geophysical Union*, 419–451.

Allan-Diaz, B. H. (1991). Water. *Table and Plant Species Relationships in Sierra Nevada Meadows: The American Midland Naturalist*, *126*(1), 30–43.

Antevs, E. (1952). Arroyo-cutting and filling. *The Journal of Geology*, *60*(4), 375–385.

Barnett, T. P., Adam, J. C., & Lettenmaier, D. (2005). Potential impacts of a warming climate on water availability in snow dominated regions. *Nature*, *438*, 303–309.

Barnett, T. P., Pierce, D. W., Hidalgo, H. G., Bonfils, C., Santer, B. D., Das, T., … Mirin, A. A. (2008). Human-induced changes in the hydrology of the Western United States. *Science*, *319*(5866), 1080–1083.

Barry, D. A., Parlange, J. Y., Sander, G. C., & Sivaplan, M. (1993). A class of exact solutions for Richards' equation. *Journal of Hydrology*, *142*(1–4), 29–46.

Bear, J. (1972). *Dynamics of fluids in porous media*. New York: American Elsevier.

Beechie, T., Sear, D. A., Olden, J. D., Pess, G. R., Buffington, J. M., Moir, H., … Pollock, M. M. (2010). Process-based principles for restoring river ecosystems. *BioScience*, *60*(3), 209–222.

Benoit, T., & Wilcox, J. (1997). *Applying a fluvial geomorphic classification system to watershed restoration*. US Department of Agriculture Forest Service: Stream Notes.

Birkeland, P. W., & Janda, R. J. (1971). Clay mineralogy of soils developed from Quaternary deposits of the eastern Sierra Nevada, California. *Geological Society of America Bulletin*, *82*(9), 2495–2514.

Brinson, M. M. (1993). *A hydrogeomorphic classification for wetlands: Wetlands research program technical report WRP-DE-4*. Vicksburg, MS: U.S. Army Corps of Engineers Waterways Experiment Station.

Brutsaert, W. (2005). *Hydrology: An introduction*. Cambridge: Cambridge University Press.

Brutsaert, W., & Nieber, J. L. (1977). Regionalized drought flow hydrographs from a mature glaciated plateau. *Water Resources Research*, *13*(3), 637–643.

Bull, W. B. (1997). Discontinuous ephemeral streams. *Geomorphology*, *19*(3–4), 227–276.

Cayan, D. R., Dettinger, M. D., Kammerdiener, S. A., Caprio, J. M., & Peterson, D. H. (2001). Changes in the onset of spring in the Western

United States. *Bulletin of the American Meteorological Society*, *82*(3), 399–415.

Cooper, D. J., Sanderson, J. S., Stannard, D. I., & Groeneveld, D. P. (2006). Effects of long-term water table drawdown on evapotranspiration and vegetation in an arid region phreatophyte community. *Journal of Hydrology*, *325*(1), 21–34.

Dyksterhuis, E. L. (1981). *Soil survey of Grant County*. Central Part: Oregon.

Essaid, H. I., & Hill, B. R. (2014). Watershed-scale modeling of streamflow change in incised montane meadows. *Water Resources Research*, *50*(3), 2657–2678.

Fryjoff-Hung, A., & Viers, J. H. (2013). *Sierra Nevada meadow hydrology assessment: Final project report to the USDA Forest Service Pacific southwest region*. Davis: University of California. 1114 p

Germanoski, D., & Miller, J. R. (2004). *Basin sensitivity to channel incision in response to natural and anthropogenic disturbance* (pp. 88–123). Great Basin Riparian Ecosystems: Ecology, Management and Restoration, Island Press, Covelo, Ca, USA.

Hammersmark, C. T., Dobrowski, S. Z., Rains, M. C., & Mount, J. F. (2010). Simulated effects of stream restoration on the distribution of wet-meadow vegetation. *Restoration Ecology*, *18*(6), 882–893.

Hammersmark, C. T., Rains, M. C., & Mount, J. F. (2008). Quantifying the hydrological effects of stream restoration in a montane meadow, Northern California, USA. *River Research and Applications*, *24*(6), 735–753.

Hammersmark, C. T., Rains, M. C., Wickland, A. C., & Mount, J. F. (2009). Vegetation and water-table relationships in a hydrologically restored riparian meadow. *Wetlands*, *29*(3), 785–797.

Harvey, M. D., & Watson, C. C. (1986). Fluvial processes and morphological thresholds in incised channel restoration. *Journal of the American Water Resources Association*, *22*(3), 359–368.

Heede, B. H. (1979). Deteriorated watersheds can be restored: A case study. *Environmental Management*, *3*(3), 271–281.

Henery, R., Purdy, S., Williams, J., Hatch, J., Fesenmyer, K., Drew, M., … Knight, C. (2011). *Meadow restoration to sustain stream flows and native trout: A novel approach to quantifying the effects of meadow restorations to native trout: Report to National Fish and Wildlife Foundation*

Klein, L. R., Clayton, S. R., Alldredge, J. R., & Goodwin, P. (2007). Long-term monitoring and evaluation of the lower red river meadow restoration project, Idaho, U.S.A. *Restoration Ecology*, *15*(2), 223–239.

Knowles, N., & Cayan, D. R. (2002). Potential effects of global warming on the Sacramento/San Joaquin watershed and the San Francisco estuary: Geophysical Research Letters, v. 29, no. 18, p. In *38–31–38-34* (Vol. 29) (pp. 38-1–38-4).

Koehler, P. A., & Anderson, R. S. (1994). Paleoecology and stratigraphy of Nichols Meadow, Sierra National Forest, California, USA. *Palaeogeography*, *Palaeoclimatology*, *Palaeoecology*, *112*(1–2), 1–17.

Lautz, L. K. (2007). Estimating groundwater evapotranspiration rates using diurnal water-table fluctuations in a semi-arid riparian zone. *Hydrogeology Journal*, *16*(3), 483–497.

Liang, L., Kavvas, M. L., Chen, Z. Q., Anderson, M., Ohara, N., Wilcox, J., & Mink, L. (2007). Modeling river restoration impact on flow and sediment in a California watershed. *In Proceedings ASCE World Environmental and Water Resources Congress, Tampa, Florida, May*, *2007*.

Lindquist, D. S., & Wilcox, J. (2000). New concepts for meadow restoration in the northern Sierra Nevada. *Proceedings of the International Erosion Control Association*, *31*(p), 145–152.

Loheide, S. P. (2008). A method for estimating subdaily evapotranspiration of shallow groundwater using diurnal water table fluctuations. *Ecohydrology*, *1*(1), 59–66.

Loheide, S. P., & Gorelick, S. M. (2005). A high-resolution evapotranspiration mapping algorithm (ETMA) with hydroecological applications at riparian restoration sites. *Remote Sensing of Environment*, *98*, 182–200.

Loheide, S. P., and Gorelick, S. M. (2006). Quantifying stream-aquifer interactions through the analysis of remotely sensed thermographic profiles and in situ temperature histories. *Environmental Science and Technology*, *40*(10), 3336–3341.

Loheide, S. P., and Gorelick, S. M. (2007). Riparian hydroecology: A coupled model of the observed interactions between groundwater flow and meadow vegetation patterning;*Water Resources Research*, *43*(7), n/a-n/a.

Lowry, C. S., Deems, J. S., Loheide, S. P., & Lundquist, J. D. (2010). Linking snowmelt-derived fluxes and groundwater flow in a high elevation meadow system, Sierra Nevada Mountains, California. *Hydrological processes*, *24*(20), 2821–2833.

Lowry, C. S., & Loheide, S. P. (2010). Groundwater-dependent vegetation: Quantifying the groundwater subsidy. *Water Resources Research*, *46*(6).

Lowry, C. S., Loheide, S. P., Moore, C. E., & Lundquist, J. D. (2011). Groundwater controls on vegetation composition and patterning in mountain meadows. *Water Resources Research*, *47*(10).

NFWF. (2010). Sierra Nevada meadow restoration, National Fish and Wildlife Foundation business plan, 38 pp. http://www.nfwf.org/sierranevada/documents/sierra_meadow_restoration_business_plan.pdf

Nolin, A. W., & Daly, C. (2006). Mapping "at risk" snow in the Pacific Northwest. *Journal of Hydrometeorology*, *7*, 1164–1171.

Ohara, N., Kavvas, M. L., Chen, Z. Q., Liang, L., Anderson, M., Wilcox, J., & Mink, L. (2014). Modelling atmospheric and hydrologic processes for assessment of meadow restoration impact on flow and sediment in a sparsely gauged California watershed. *Hydrological processes*, *28*(7), 3053–3066.

Palmer, M. A., Lettenmaier, D. P., Poff, N. L., Postel, S. L., Richter, B., & Warner, R. (2009). Climate change and river ecosystems: Protection and adaptation options. *Environmental Management*, *44*(6), 1053–1068.

Payne, J. T., Wood, A. W., Hamlet, A. F., Palmer, R. N., & Lettenmaier, D. P. (2004). Mitigating the effects of climate change on the water resources of the Columbia River basin. *Climatic Change*, *62*(1), 233–256.

Peacock, K. A.. (1994). Valley fill and channel incision in Meyer's Canyon, northcentral Oregon [M.S.]: Oregon State University, 165 p.

Pilliod, D. S., Rohde, A. T., Charnley, S., Davee, R. R., Dunham, J. B., Gosnell, H., … Nash, C. (2018). Survey of beaver-related restoration practices in rangeland streams of the Western USA. *Environmental management*, *61*(1), 58–68.

Podolak, K., Edelson, D., Kruse, S., Aylward, B., Zimring, M., & Wobbrock, N. (2015). *Estimating the water supply benefits from forest restoration in the northern Sierra Nevada: The nature conservancy*.

Poff, N. L. (2002). Ecological response to and management of increased flooding caused by climate change. *Philosophical Transactions of the Royal Society of London A: Mathematical, Physical and Engineering Sciences*, *360*(1796), 1497–1510.

Pollock, M. M., Beechie, T. J., Wheaton, J. M., Jordan, C. E., Bouwes, N., Weber, N., & Volk, C. (2014). Using beaver dams to restore incised stream ecosystems. *BioScience*, *64*(4), 279–290.

Ponce, V. M., & Lindquist, D. S. (1990). Management of baseflow augmentation: A review. *Journal of the American Water Resources Association*, *26*(2), 259–268.

Ramstead, K. M., Allen, J. A., & Springer, A. E. (2012). Have wet meadow restoration projects in the Southwestern U.S. been effective in restoring geomorphology, hydrology, soils, and plant species composition?: *Environmental Evidence*, *1*(11), 1–sd16.

Ratliff, R. D. (1985). Meadows of the Sierra Nevada of California: State of knowledge: Gen. Tech. Rep. PSW-84 Berkeley, CA, Pacific Southwest Forest and Range Experiment Station, Forest Service, U.S. Department of Agriculture, 52 p.

Readle, J. R. (2014). Groundwater storage potential in degraded meadows along Last Chance Creek, Plumas County, California PhD: California State University, Sacramento.

Richards, L. A. (1931). Capillary conduction of liquids through porous mediums. *Physics*, *1*, 318–333.

Roni, P., Hanson, K., & Beechie, T. (2008). International review of effectiveness of stream rehabilitation. *North American Journal of Fisheries Management*, *28*, 856–890.

Rosgen, D. L. (1997). A geomorphological approach to restoration of incised rivers, proceedings of the conference on management of landscapes disturbed by channel incision, v. 16.

Rupp, D. E., & Selker, J. S. (2005). Drainage of a horizontal Boussinesq aquifer with a power law hydraulic conductivity profile: *Water Resources Research*, *41*(11), n/a-n/a.

Safeeq, M., Grant, G., Lewis, S., & Tague, C. (2013). Coupling snowpack and groundwater dynamics to interpret historical streamflow trends in the Western United States. *Hydrological Processes*, *27*(5), 655–668.

Safeeq, M., Shukla, S., Arismendi, I., Grant, G. E., Lewis, S. L., & Nolin, A. W. (2015). Influence of winter season climate variability on snow-precipitation ratio in the Western U.S. *International Journal of Climatology*.

Sauer, V. B., & Meyer, R. W. (1992). *Determination of error in individual discharge measurements* (pp. 4–7). Denver, CO: U.S. Geological Survey.

Seager, R., & Vecchi, G. A. (2010). Greenhouse warming and the 21st century hydroclimate of southwestern North America. *Proccedings of the National Academy of Sciences*, *107*(50), 21277–21282.

Shields, F. D., Knight, S. S., & Cooper, C. M. (1995). Incised stream physical habitat restoration with stone weirs: Regulated rivers. *Research & Management*, *10*(2–4), 195.

Simon, A., Curini, A., Darby, S. E., & Langendoen, E. J. (2000). Bank and near-bank processes in an incised channel. *Geomorphology*, *35*(3), 193–217.

Stewart, I., Cayan, D. R., & Dettinger, M. (2004). Changes in snowmelt runoff timing in western North America under a "business as usual" climate change scenario. *Climatic Change*, *62*, 217–232.

Swanson, S., Franzen, D., & Manning, M. (1987). Rodeo Creek: Rising water on the high desert. *Journal of Soil and Water Conservation*, *42*(6), 405–407.

Tague, C., & Grant, G. E. (2009). Groundwater dynamics mediate low-flow response to global warming in snow-dominated alpine regions. *Water Resources Research*, *45*(7).

Tague, C., Valentine, S., & Kotchen, M. (2008). Effect of geomorphic channel restoration on streamflow and groundwater in a snowmelt-dominated watershed: *Water Resources Research*, v. *44*, no. 10, p. N/a-n/a, 44.

USDA. (2013). Ecological restoration implementation plan: Forest Service Pacific Southwest Region, report R5-MB-259

Walter, R. C., & Merritts, D. J. (2008). Natural streams and the legacy of water-powered mills. *Science*, *319*(5861), 299–304.

White, W. N. (1932). A method of estimating ground-water supplies based on discharge by plants and evaporation from soil; results of investigations in Escalante Valley, Utah, Washington, D.C., US Government Printing Office. *Water Supply Paper*, *659-A*, 105.

Wood, S. H. (1975). Holocene stratigraphy and chronology of mountain meadows, Sierra Nevada, California [Ph.D.: California Institute of Technology, 204 p.

How to cite this article: Nash CS, Selker JS, Grant GE, Lewis SL, Noël P. A physical framework for evaluating net effects of wet meadow restoration on late-summer streamflow. *Ecohydrology*. 2018;e1953. https://doi.org/10.1002/eco.1953